Hindawi
International Journal of Photoenergy
Volume 2019, Article ID 1812879, 16 pages
https://doi.org/10.1155/2019/1812879

Review Article

Recent Progress of Graphene-Based Photoelectrode Materials for Dye-Sensitized Solar Cells

Kaustubh Patil,[1] Soheil Rashidi,[1] Hui Wang,[2] and Wei Wei[1]

[1]*Mechanical Engineering Department, Wichita State University, 1845 Fairmount Street, Wichita, KS 67260, USA*
[2]*Mechanical Engineering Department, Conn Center for Renewable Energy Research, University of Louisville, 332 Easter Parkway, Louisville, Kentucky 40292, USA*

Correspondence should be addressed to Wei Wei; wei.wei@wichita.edu

Received 14 September 2018; Revised 23 December 2018; Accepted 12 February 2019; Published 26 March 2019

Academic Editor: Leonardo Palmisano

Copyright © 2019 Kaustubh Patil et al. This is an open access article distributed under the Creative Commons Attribution License, which permits unrestricted use, distribution, and reproduction in any medium, provided the original work is properly cited.

Graphite with a single atomic layer known as graphene shows great capability in energy conversion and storage devices. Dye-sensitized solar cells (DSSCs) have attracted intense interests due to offering high photo-to-electric conversion efficiencies. DSSCs are built from a photoelectrode (a dye-sensitized nanocrystalline semiconductor), an electrolyte with redox couples, and a counterelectrode. In this review article, we outline the strategies to enhance the efficiency and reduce the cost by introducing graphene into the DSSCs as the photoelectrode. First, the development of DSSCs and the properties of graphene are briefly described. Then, the applications of graphene-based materials for photoelectrodes (transparent electrode, semiconductor layer, and dye sensitizer) in DSSCs are deeply discussed. Finally, an outlook for graphene materials in DSSCs is provided.

1. Introduction

Finding an alternative option of energy has become today's essential need, with depleting conventional resources of energy, such as fossil fuels. Solar energy, as the largest single available source of clean energy, has the potential to overcome this problem. Solar cells provide an efficient method to convert solar energy into electricity [1]. The first-generation solar cells are made of ultrapure silicon metal. However, the production of ultrapure Si requires high energy, leading to the cost of electricity produced by this technology which is several times higher than that produced from fossil fuels [2]. One of the alternatives for the Si solar cells is dye-sensitized solar cell (DSSC), because of their relatively high photo-to-electric conversion efficiencies, low production cost, and environmental benignity [3, 4]. DSSC basically consists of three components, including photoelectrode, electrolyte, and counterelectrode. O'Regan and Grätzel established the state-of-the-art DSSCs: a dye-sensitized nanocrystalline TiO_2 film as photoelectrode, I_3^-/I^- redox ?couple as electrolyte, and Pt as counterelectrode [5, 6]. Applications of new materials have been explored to enhance the efficiency and reduce the basic cost of DSSCs.

1.1. Dye-Sensitized Solar Cells (DSSCs). DSSCs are also known as Grätzel solar cells, honoring their invention and the pioneering work. Figure 1 shows a schematic representation of a DSSC, including a photoelectrode, a photosensitizer, an electrolyte, and a counterelectrode [7]. A DSSC has three important steps through which it converts sunlight into electrical energy: when sunlight falls on a dye, it starts the photoexcitations and makes electrons to move to the semiconductor's conduction band. Dye molecules are oxidized back by electrons given by electrolyte through redox reaction and finally travel through the external load electrons to complete the circuit. A number of reviews and book chapters on DSSCs have been published in the literature [8–11]. The electrochemistry, physics, materials science, and technology behind DSSCs have been extensively reviewed therein by leading professionals working in this field. In this review article, we are going to review the latest developments of graphene photoelectrode materials.

1.1.1. The Function of Photoelectrode and Its Requirements. The photoelectrode is a mesoporous oxide layer composed of nanometer-sized particles with a monolayer of dye

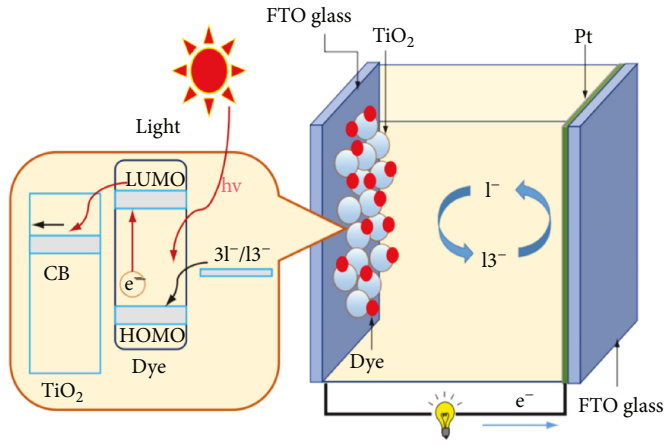

Figure 1: Scheme diagram of dye-sensitized solar cells [7].

attached to the surface, which is responsible for light absorption. It is an important component in DSSC, as it converts photons into electrical energy [12, 13]. It can strongly influence the photovoltage, the fill factor, and the photon-to-current conversion efficiency (IPCE). The process can be described as follows: when exposed to sunlight, the electrons of the dye are first excited from the highest occupied molecular orbital (HOMO) to the lowest unoccupied molecular orbital (LUMO) [14]. Then they are transferred to the semiconductor's conduction band and passed from the semiconductor network, being accumulated at the transparent conducting oxide. An electrolyte solution which typically consists of an iodide/triiodide redox couple donates electrons to regenerate the oxidized dye. At last, the electrons transport to the counterelectrode through the external circuit and reduce the triiodide ions back to the iodide to complete the process. A good photoelectrode is supposed to provide good electron injection, good electron collection, and good usage of light. Many different materials have been explored as photoelectrode in DSSCs. Among them, titanium dioxide (TiO_2) powder is most abundantly used because of the low recombination rate for the hole-electron pair and great absorption property [15]. Moreover, ZnO which has a very high electron movability has also gathered so much attention to be employed as photoelectrode materials in DSSCs [16–36].

1.2. Graphene. Graphene, one of the allotropes of abundantly available carbon, has emerged as one of the most promising materials for applications in solar cells. It was first discovered in 2004 by Novoselov et al. [37] and awarded with a Nobel prize in 2010 [38–40]. Graphene is a 1-atom-thick transparent layer of sp^2-hybridized carbon atoms packed into a 2D nanostructure (Figure 2) [39]. The related structures include fullerene, carbon nanotubes, and graphite (Figure 2). Graphene possesses high carrier mobility, low sheet resistance, and high optical transparency, which would constitute its excellent candidate as an electrode material [37]. Another unique property graphene has is that it can repair holes in the sheet by itself when it is exposed to the molecules containing carbon atoms [41]. Carbon atoms align themselves in a hexagonal lattice perfectly. Pristine graphene has no bandgap; therefore, it acts as a semimetal [42]. Currently available methods aiming for pristine graphene include mechanical exfoliation [43] and liquid exfoliation. However, both of them have low production. Scientists are exploring new chemical and physical ways to create an artificial bandgap in graphene, which is one of the requirements for the fabrication of electronic devices. Zero-bandgap graphene can be transformed into a wide-bandgap semiconductor through hydrogenation via sp^3 C–H bond formation [44].

Because graphene is an atom-thick layer [45], it is a perfect nanoscale material and, therefore, has great potential in a very wide range of applications in the field of nanotechnology, including nanoelectronics, nanooptics, display devices, LEDs, computer data storage, energy, membranes, nanofilters for water purification, sensors, nanomedicine, stem cells, and energy conversion devices [46–50], such as DSSCs [51–56]. Graphene possesses a lamellar structure and high conductivity, which can help to improve the conductivity and increase the photovoltaic efficiency of DSSCs (5.98%) when introduced to MoS_2 [57]. Graphite paper is another form of graphene. It is very lightweight and has a flexible structure which is good for mass production and for use in DSSCs [58]. Reduced graphene oxide (rGO) is an intermediate stage of graphene oxide and graphene, and it has various types of oxygen-containing functional groups, like –OH, =O, and –COOH, and lattice surface defects which generate the electrocatalytic site in metal nanoparticles. This is why rGO showed much better performance than the fully reduced defect-free graphene [59]. Graphene nanoplatelets (GNP) have been explored as counterelectrodes because of their higher active sites, such as edge defects and oxide groups [60].

1.2.1. Preparation of 2D Graphene. In order to reach a high mass production capability and understand the process which involves a solution or thin film basis, numerous efforts have been developed to synthesize graphene and its derivatives. These processes are usually differentiated in two categories: the bottom-up and top-down approaches. Graphene materials can be directly synthesized from the carbon sources

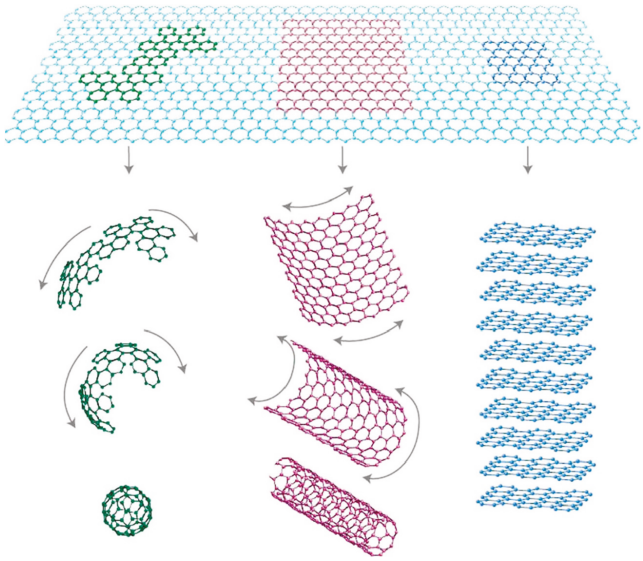

Figure 2: Graphene (top) and related structure: fullerene (bottom left), carbon nanotubes (bottom center), and graphite (bottom right) [39].

in a bottom-up approach. For example, chemical vapor deposition (CVD) is a generally bottom-up process used to develop large-area, single, and few-layer graphene sheets on metal substrates [61–64]. Another example is the plasma-enhanced CVD (PECVD). The difference between PECVD and CVD is that this method can develop one-layer graphene in large quantity at a lower deposition temperature and in a shorter reaction time. Besides, single-layer and few-layer graphene films can also be obtained via the graphitization of carbon-containing substrates, such as SiC, through high-temperature annealing [65, 66]. In addition to these solid-phase deposition methods, wet chemical reaction of ethanol and sodium followed by pyrolysis is another method to synthesis graphene [67], or graphene-like polyaromatic hydrocarbons through organic synthesis [68, 69]. Figure 3(a) shows the electrical characteristics of the as-prepared transparent carbon films via a new bottom-up chemical approach involving the thermal reaction of synthetic nanographene molecules of giant polycyclic aromatic hydrocarbons which are cross-linked with each other and further fused into larger graphene sheets (Figure 3(b)). A small decrease in the film conductivity was observed as the film thickness decreased. The structure of the graphene film, as shown in Figure 3(c), consisted of ordered, tightly packed graphene layers. As illustrated in Figures 3(d) and 3(e), graphene film shows an ultrasmooth surface compared with the relatively rough surface and chemical instability of ITO [68].

Compared with the bottom-up approaches, the top-down approaches show great potentials, such as high yield, liquid-based processability, and less complicated execution. Intercalation, chemical functionalization, sonication of bulk graphite, and electrochemical exfoliation of graphite have been demonstrated as top-down approaches [70]. However, there are some drawbacks of top-down methods, such as low yield of single-layer production [71], expensive intercalates [72], and residual surfactant-induced low conductivity. Therefore, the reduction of highly oxidized graphene oxide (GO) sheets from the exfoliated graphite oxide has been developed as an alternative approach [73]. The reaction of graphite with a mixture of potassium permanganate (KM nO_4) and concentrated sulfuric acid (H_2SO_4) is usually referred to as Hummers' method. Graphite oxide can be obtained by this method [74, 75]. The surfaces of exfoliated GO sheets are thus highly oxidized and featured with the residual epoxides, hydroxides, and carboxylic acid groups [76, 77]. Till date, rGO sheets can be obtained by various types of reduction methods, such as chemical reagent reduction [78–86], photochemical reduction [87–90], microwave-assisted reduction [91], thermal reduction [92–98], photothermal reduction [99, 100], and electrochemical reduction [101–103]. Many reduction agents were employed in the chemical reduction process, such as hydrazine [104], strong alkaline media [83], vitamin C or ascorbic acid [105], bovine serum albumin (BSA) [85], bacterial respiration [106], and hydriodic acid [107]. Hydriodic acid is used to change the hydrazine reduction from the reaction of making rGO thin films due to its low toxicity. Although rGO has more charge-transfer resistance than pure graphene because of defects and the presence of residual oxygenated groups, the tenability in electronic and optoelectronic properties via chemical reactions [108] and the feasibility for composite incorporation [109] can be provided by the reactive surfaces.

1.2.2. Preparation of 3D Graphene. There are various requirements according to different applications to satisfy them; three-dimensional (3D) graphene with various morphologies, structures, and properties was designed and synthesized via numerous methods.

There are various strategies used, but self-assembly is one of the most common for bottom-up nanotechnology. Graphene naturally becomes a versatile nanoscale building block for self-assembly to achieve hierarchical microstructures and novel functionalities due to its unique structure and properties [110]. One very common example for producing 3D graphene structures is through the gelation process of GO dispersion followed by reduction to convert GO to rGO [111]. The lyophilized GO dispersion shows a 3D network composed of GO sheets, as shown by its SEM images (Figure 4). GO sheets can be nicely distributed in water-based solvent because of the force balance between the van der Waals attractions from the basal planes of GO sheets and the electrostatic repulsions from the functional groups of GO sheets. Once this force balance is broken, gelation of GO dispersion occurs. During the gelation process to form a 3D design of GO hydrogels, GO sheets overlap each other a little bit. 3D rGO networks are obtained after further reduction of the GO hydrogels. Many methods have been employed to initiate the gelation of GO dispersion, for example, addition of cross-linkers [112], change in the pH value of the GO dispersion [112], or ultrasonication of the GO dispersion [113]. In the meantime, so many other materials have also been explored as cross-linkers for the self-assembly of GO sheets, such as DNA [114], metal ions [115–117], polymers [118], and organic molecules [119]. In addition to the gelation process of a GO dispersion, other methods such as

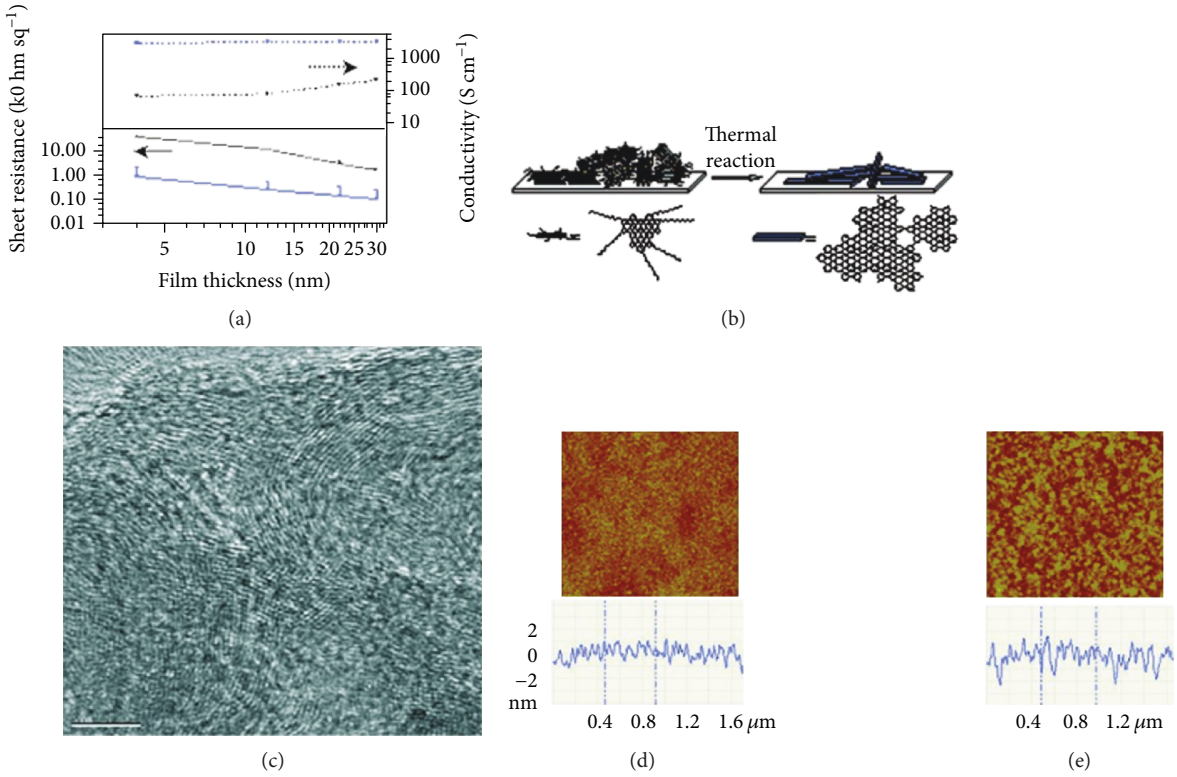

Figure 3: (a) Sheet resistance (solid curves with half error bars in the plus direction) and corresponding average conductivity (short dashed curves) of the transparent graphene films (TGFs) as a function of the film thickness, with the plot in the log-log scale. Black and blue curves denote the TGFs produced on quartz and SiO_2/Si, respectively. (b) Illustration of the mechanism of the intermolecular condensation of nanographene 1 into graphitic networks. (c) A representative HRTEM image of a TGF (scale bar: 5 nm). (d) and (e) AFM height images ($2 \times 2\ \mu m^2$) of 4 and 30 nm thick TGF surfaces, respectively (color scale: black to bright yellow, 10 nm). Each image is accompanied with a cross-sectional plot which has the same vertical scale [68].

freeze-drying [120], tape casting [121], controlled filtration [122], centrifugation of GO dispersions [123], electrochemical deposition [124], and sol-gel reaction [125, 126] have also been employed to obtain 3D graphene materials.

Another method that can prepare 3D graphene is called the template-assisted method. The advantage of this method is that it can obtain 3D graphene with much more controlled morphologies and properties because of the use of predesigned 3D templates, such as CVD methods [127–129]. For example, 3D graphene networks were successfully synthesized by using commercially available Ni foam as both template and catalyst [127]. The synthesis of graphene foam and its integration with polymers are illustrated in Figure 5. The authors chose nickel foam, a porous structure with an interconnected 3D scaffold of nickel, as a template for the growth of graphene foam. Then, carbon was introduced into a nickel foam by decomposing CH_4 at 1000°C under ambient pressure, and graphene films were then precipitated on the surface of the nickel foam. Besides the Ni foam mentioned before, anodic aluminum oxide [130], MgO [131], nickel-coated pyrolyzed photoresist film [132, 133], metal nanostructures [134, 135], and metallic salts [136] have also been used as templates to synthesize 3D graphene.

In addition, the direct deposition of 3D graphene architectures by plasma-enhanced CVD (PECVD) methods [137–139] is a straightforward strategy, in which Au and stainless steel have been employed. 3D graphene was formed since the graphene sheets were vertically grown on the substrate and connected with each other. As a result, the materials obtained by this method firmly adhered to the substrate.

2. Graphene Photoelectrode Applications

The photoelectrode of a DSSC is usually made from transparent conducting glass or plastic substrate on which a dye-sensitized TiO_2 layer is coated. It is important to increase the loading of dye molecules, enlarge the interface area of the dye/electrolyte, and improve the conductivity of electrons at the semiconductor layer to compete with charge recombination. Graphene possesses excellent properties like high transparency, good thermal stability, high room temperature carrier mobility, and low impedance level, which have attracted great attention [140]. Recently, in photoelectrodes graphene material also has been explored as transparent conductors, as electron promoter in the semiconductor layer, and as additive in dye sensitizers.

2.1. Transparent Electrode. Indium tin oxide (ITO) material has high conductivity and very high transmittance in the visible spectrum, and that is why it is used as transparent electrode much widely. But the problem with the ITO material is that it is brittle and unstable at high temperature. So that

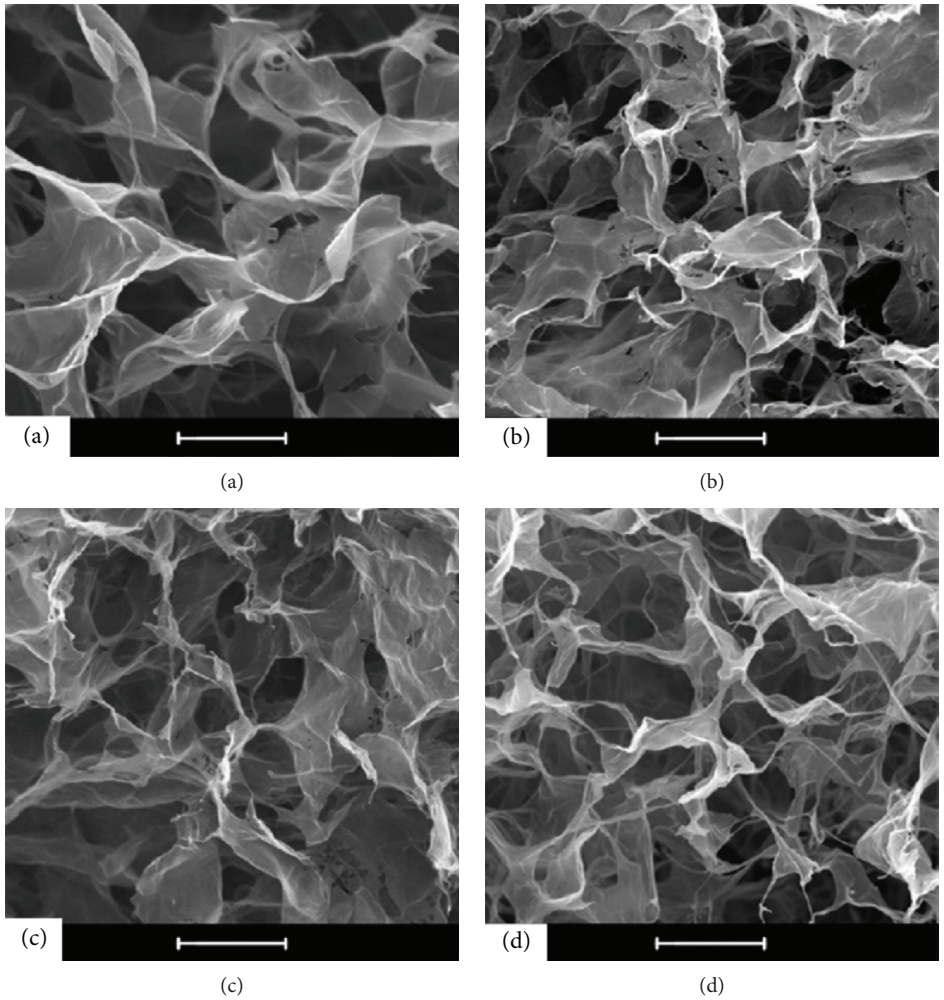

Figure 4: SEM images of lyophilized GO solution and three typical GO hydrogels: (a) GO solution, (b) GO/PVP hydrogel with 1 mg mL^{-1} PVP, (c) GO/PDDA hydrogel with 0.1 mg mL^{-1} PDDA, and (d) GO/Ca^{2+} hydrogel with 9 mM Ca^{2+}. C_{GO} = 5 mg mL^{-1}, and scale bar = 10 μm [111].

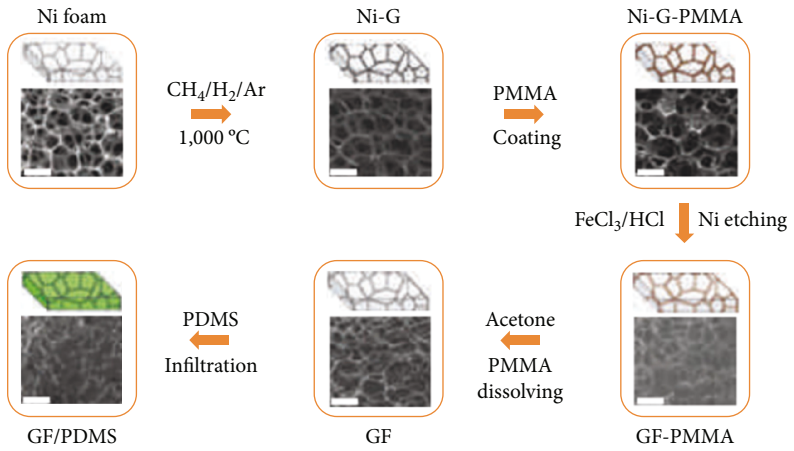

Figure 5: Synthesis of a GF and integration with PDMS. (a) A nickel (Ni) foam. (b) CVD growth of graphene films (Ni–G) using Ni foam as a 3D scaffold template. (c) An as-grown graphene film after coating a thin PMMA supporting layer (Ni–G-PMMA). (d) A GF coated with PMMA (GF-PMMA) after etching the nickel foam with hot HCl (or $FeCl_3$/HCl) solution. (e) A free-standing GF after dissolving the PMMA layer with acetone. (f) A GF/PDMS composite after infiltration of PDMS into a GF. All the scale bars are 500 μm [127].

is why graphene has been coming out as an alternative material which has a low cost and has better properties than the ITO material without any limitations [141].

Wang et al. were the first ones to make a transparent and conductive graphene electrode in 2008 for DSSCs [142]. The graphene films were fabricated via the exfoliation of graphite oxide and thermal reduction of the resultant platelets. As the transparent electrode, solid-state DSSCs based on spiro-OMeTAD and porous TiO_2 were fabricated as shown in Figure 6. The work function of graphene is lower than that of the counter gold electrode, therefore qualifying for application as the transparent anode in the DSSCs as indicated in Figure 6(a). An efficiency of 0.26% was obtained when a graphene film with a Rs of 1.8 kΩ/sq and transmittance of 72% (550 nm) was used as anode electrode. The low efficiency of DSSC was claimed to be due to the low quality of the graphene film [142]. Furthermore, few-layer graphene films on SiO_2 substrates were prepared by Huang et al. by using ambient pressure chemical vapor deposition. The prepared graphene films achieved a power conversion efficiency of 4.25% which is not so much different from those FTO counterelectrodes [143].

2.2. Semiconducting Layer. To increase the performance of the DSSC nowadays, graphene has been added to the semiconductor which improves the charge collection [144–146]. The work function of graphene, which is about -4.4 eV, is between the conduction band of TiO_2 and the work function of ITO. This benefits in suppressing the charge recombination by fast collection of the electrons at the anode [147]. On the other hand, visible light irradiation can excite the valence electrons from graphene into the TiO_2 conductive band at the graphene/TiO_2 interface based on a theoretical study [148], which results in separated electron-hole pairs. In addition, the conductive percolation threshold of the graphene/TiO_2 layer is only at 1 vol% of the graphene loading [149]. However, transmittance of the composite film decreases with increasing the graphene content; hence, to have a maximum efficiency, the optimal value needs to be obtained [149, 150]. Besides the enhanced conductivity, the large surface area of graphene improves the loading and dispersion of the dye molecules. Graphene processes a theoretical surface area of 2630 $m^2 g^{-1}$, which shows great potential as an ideal support material with enhanced interfacial contact even when used in small amounts [151]. It is reported that graphene surfaces can bind with dye molecules, such as porphyrin. Then, the photocurrent will be generated when photoirradiation undergoes energy and electron transfer [152]. Moreover, the light scattering at the photoanode can also be enhanced by forming a graphene/TiO_2 composite porous network [149]. Consequently, by using graphene/-TiO_2 as the photoanode, efficiency was increased by 39% higher than using commercial P25 TiO_2 which is 4-7% [149].

There are so many ways through which graphene has been incorporated into the semiconductor film. Kim et al. reported the UV-assisted photocatalytic reduction of graphene oxide/TiO_2 nanoparticles. In the gap of FTO and nanocrystalline TiO_2, the prepared graphene/TiO_2 was applied as an interfacial layer [153]. Because of the lower roughness of graphene-TiO_2, it provided much better adhesion than did the normal interfacial layer between FTO and TiO_2. The solar cell showed a PCE of 5.26%, which is higher than that without a blocking layer (PCE = 4.89%). Chen et al. also used a similar kind of method to increase the performance of the DSSCs. They spin-coated the graphene on the FTO which helps in preventing the recombination of the charge between FTO and TiO_2 [144]. Because of this, efficiency improved marginally from 5.80% to 8.13%.

Graphene could also be used as a current collector. Yang et al. incorporated 2D graphene into the TiO_2 nanostructure, aiming at increasing light collection, preventing charge recombination, and thus enhancing the charge transportation rate [154]. Bavir and Fattah employed a composite of TiO_2 and graphene as photoelectrode to replace the TiO_2-ZnO composite [18]. DSSC with TiO_2-graphene as photoelectrode shows a higher efficiency of 9.3% than that (6.5%) of TiO_2-ZnO photoelectrode. Table 1 summarizes the photovoltaic characteristics of DSSCs fabricated with graphene incorporated into the semiconducting layers.

Low et al. used rGO and TiO_2 nanocomposite as photoanode [155]. They tried to find out the optimum amount of TiO_2 on the rGO photoanode for maximum efficiency. 0.3 wt% of TiO_2 on rGO showed a maximum photocurrent generation efficiency. rGO has limited capacity to absorb visible light from solar illumination, and it is only 2.3%. Adding TiO_2 enhances the capacity of rGO to absorb the light. Here, graphene oxide was synthesized through improved Hammer's method from graphite flakes. In the acids $H_2SO_4 : H_3PO_4$ (9 : 1), a mixture of graphite flakes (1.5 g) and $KMnO_4$ (9.0 g) was poured, and the reaction was carried out in cold water. The whole reaction was carried out in normal cold water (<20°C) and stirred for 24 hours. By adding 3 mL of H_2O_2 in the mixture, the oxidation process was stopped. The color of the mixture became light brownish showing a high oxidation level of graphite. GO was centrifuged to remove the supernatant. HCl and DI, remaining solid, were washed and dried in the oven for 36 hours. The dried powder is then again added with water (3 mg/mL). Then, hydrazine (1 μL for 3 mg of GO) is added to the mixture, and to add more heat, it was immersed to an oil bath, with oil at 80°C. The obtained mixture in the last was high-quality RGO. For the preparation of TiO_2, TTIP was used as precursor and the precipitation-peptization method was used. The mixture was made by adding 10 mL of TTIP and 40 mL of propanol solution then stirred for 30 minutes. Another mixture was made by adding 5 mL of acetic acid, 10 mL of propanol, and one drop of Triton X-100 into the purified water. This mixture was also stirred for 30 minutes. The first mixture was then added slowly into the second mixture with a rate of 1 mL/min. Finally, TiO_2 solution was obtained by stirring the mixture for 2 hours. Different samples were made by adding various amounts of TiO_2 (0.1, 0.2, 0.3, 0.4, and 0.5 wt% of TiO_2, respectively) solution into the RGO solution and dried into the oven for 24 hours. Samples were then calcinated at 450°C for 2 hours. Figure 7(a) shows the complete work of the DSSC schematically under a light irradiation process. At the beginning, the adsorption of a photon by N-719 dye will be transformed from the dye

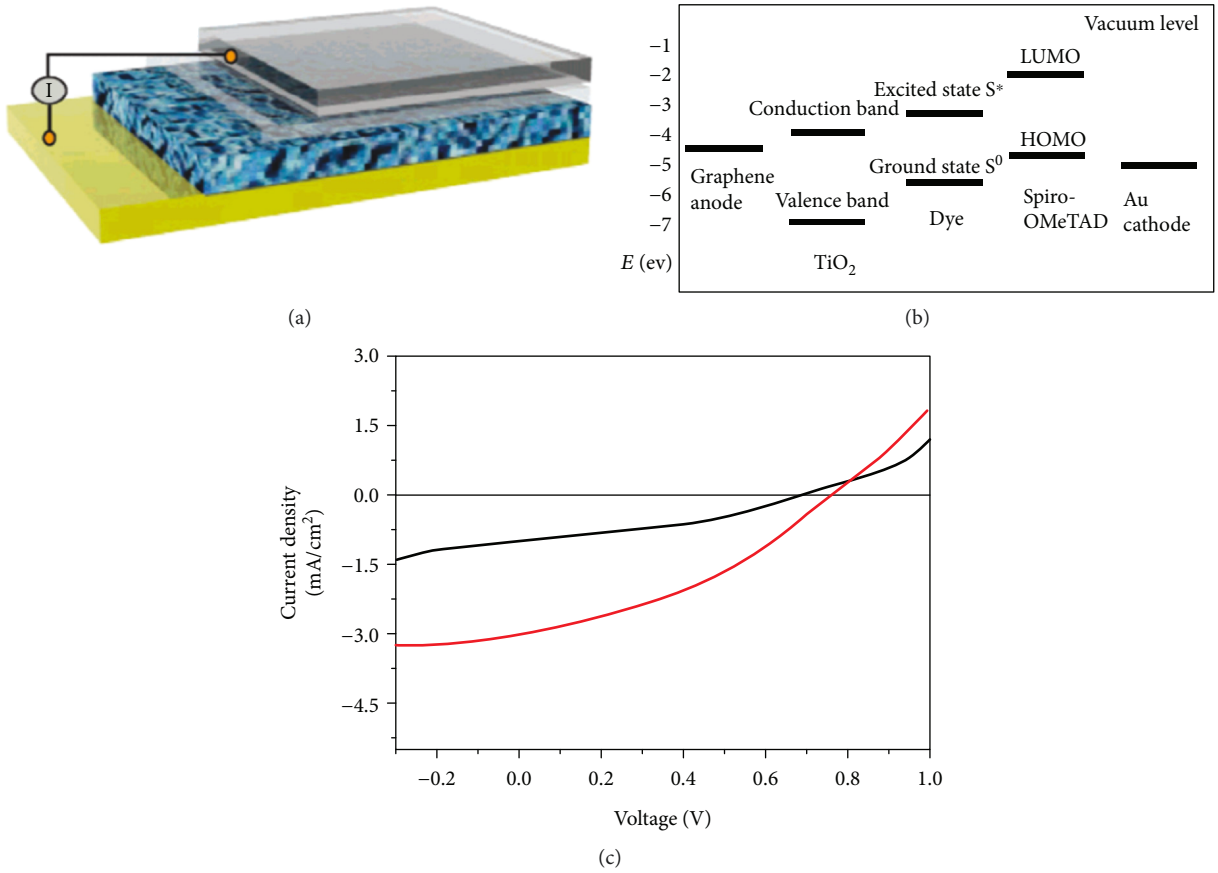

Figure 6: Illustration and performance of a solar cell based on graphene electrodes. (a) Illustration of the dye-sensitized solar cell using graphene film as electrode; the four layers from bottom to top are Au, dye-sensitized heterojunction, compact TiO_2, and graphene film. (b) The energy level diagram of the graphene/TiO_2/dye/spiro-OMeTAD/Au device. (c) I-V curve of the graphene-based cell (black) and the FTO-based cell (red), illuminated under AM solar light (1 sun) [142].

Table 1: PV characteristics of DSSCs fabricated with graphene incorporated with a semiconducting layer.

Photoelectrodes	J_{sc} (mA cm^{-2})	V_{oc} (V)	ff	η (%)	Ref.
Underlayer with RGO, scaffold layer with RGO, scattering layer with RGO	23.2	0.73	0.55	9.2	[163]
Scaffold layer with T-CRGO	8.4	0.75	0.68	4.3	[156]
Scaffold layer with CVD-derived graphene on Al_2O_3	10.2	0.78	0.68	5.4	[164]
Scaffold layer with TRGO	7.6	0.67	0.54	2.8	[146]
Scaffold with thermally treated CTAB-functionalized graphene	12.8	0.82	0.62	6.5	[165]
Scaffold layer with T-CRGO	16.3	0.69	0.62	7.0	[150]
Underlayer with T-CRGO	6.7	0.56	0.4	1.7	[147]

molecule, S, to the excited state (S*) during the harvesting of DSSCs under the irradiation with AM 1.5 condition. Then, an electron was transferred rapidly (ps or fs) to the wide bandgap semiconductor. After that, from the N-719 dye an excited electron, S*, was injected into the TiO_2–rGO photoanode while the other S* collected by FTO glass flowed through the outer circuit heading to the cathode (graphite) of the FTO glass. Finally, electrons through electrolyte redox reaction I^-/I_3^- reduce the oxidized S* to the original state. Performance of DSSC with 0.3% wt of TiO_2 and RGO photoanode has a maximum efficiency of 7.2%, with J_{sc} of 28.36 mA cm^{-2}, V_{oc} of 0.54, and ff of 0.47 (Figure 7(b)). This is mostly because of the higher probability to capture and transport the electrons from photoelectrode in a high-conductivity condition. The conductivity was maximized because of the formation between rGO and TiO_2; hence, rGO shows a very high conductivity and TiO_2 has high photocatalytic characteristic.

Tang et al. proposed a molecular grafting method to develop a photoanode where exfoliated graphene sheets (GS) are attached to a TiO_2 nanoparticle matrix in which the graphene sheets were chemically exfoliated and chemisorbed in

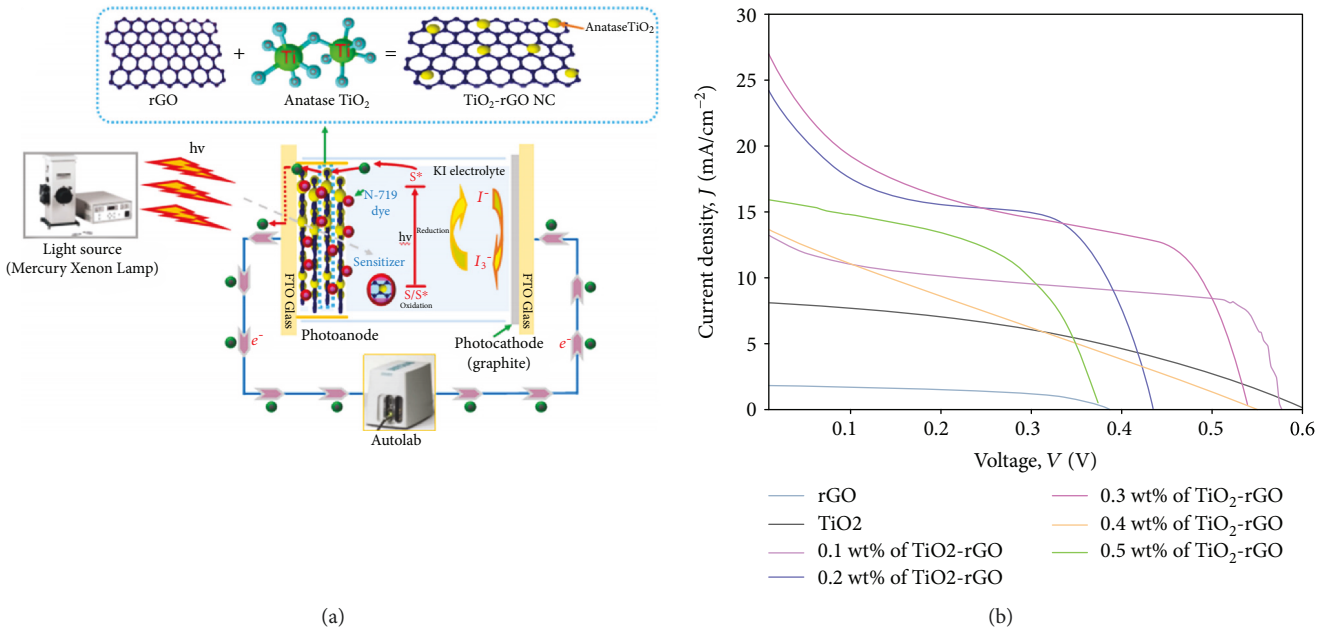

(a) (b)

Figure 7: (a) Schematic of TiO_2–rGO NC-based-DSSCs. (b) J–V curves of DSSCs under AM 1.5 condition with rGO, TiO_2, and various amounts of TiO_2–rGO [155].

the TiO_2 matrix (Figure 8) [147]. The conductivity of the reduced graphene sheets and good attachment of TiO_2 could be achieved by controlling the oxidation time of the chemical exfoliation process. It was proved that by adding the GO not only the efficient electronic transport path was provided but also the increased dye loading of the film, leading to an increase in the photocurrent. The graphene-implanted TiO_2 showed a conversion efficiency of 1.68%. Graphene was also reported to be dispersed using Nafion and then incorporated in TiO_2 particles by heterogeneous coagulation particles [156]. It is known that P25 particles and graphene process opposite zeta potentials; therefore, the TiO_2 nanoparticle binds to the surface of graphene via a strong electrostatic attractive force. The DSSC with P25 nanoparticles showed a J_{sc} of 5.04 mA cm^{-2} and PCE of 2.7%. In the presence of 0.5 wt% graphene, J_{sc} increased from 66% to 8.38 mA cm^{-2}, resulting in an efficiency of 4.28%. The authors proposed that the creation of surface morphologies increased the available sites, while electrons travel through long mean free paths without a recombination-extended electron lifetime. As a result, the performance was enhanced. Figure 9(a) shows the TEM images of graphene, which are thin, and part of them overlay while containing wrinkles and rolled edges. Figure 9(b) shows the zeta potential curves for the graphene and P25 particles in ethanol. The zeta potential of graphene is -42 mV, while that of P25 is 15 mV. Clearly, because of strong opposite potentials on both the materials, particles of P25 tend to bind on the surface of graphene. Figure 9(c) shows EIS spectra of the DSSCs using P25 and P25-graphene electrodes at an applied bias of V_{oc}. In a high-frequency region and middle-frequency region, there are two well-defined semicircles. Acceleration of the electron transfer process in the film photoanode can be seen from the reduced size of the semicircle in the high-frequency region for the P25-graphene electrode compared to the P25 electrode. As shown in Figure 9(d), The work function of graphene is in the range of 4.42-4.5. It signifies possible electrons moving from the conduction band of P25 to graphene. Then, the electrons transfer through the graphene sheets and were collected by FTO glasses.

Kilic and Turkdogan compared the results of DSSC with FTO/3D-ZnO-based photoanode and graphene/3D-ZnO--based photoanode [157]. Adding graphene increases the porosity of the photoanode which helps in increasing the charge transfer. Graphene was synthesized from the graphite by first converting it into reduced graphene oxide and then into graphene flakes by the modified Hummers' method. This graphene was then dip-coated on the FTO substrate. Then, by facile hydrothermal growth method, 3D-ZnO was grown on graphene. Efficiency of DSSC with graphene/3D-ZnO drastically increased than using pure ZnO as photoanode, which was improved from 5.117% to 6.628%. Because of the good interconnectivity and fast charge transport between graphene and the 3D-ZnO nanostructure, there is an increase by 29.4% in PCE for graphene/ZnO photoanode DSSC compared to DSSC with conventional ZnO electrode and Pt CE. It was proved that the graphene layer increased the external quantum efficiency with more charge carrier collection through a better aligned band structure, which reduces the charge recombination rate.

2.3. Dye Sensitizer. There are two requirements for an effective sensitizer of a DSSC: (1) it should have the capability to absorb a wide range of solar spectrum, and (2) electrons must be quickly moved to the semiconductor scaffold from the ground state. Traditionally, ruthenium polypyridyl and quantum dots are used as sensitizers in the photoanode for

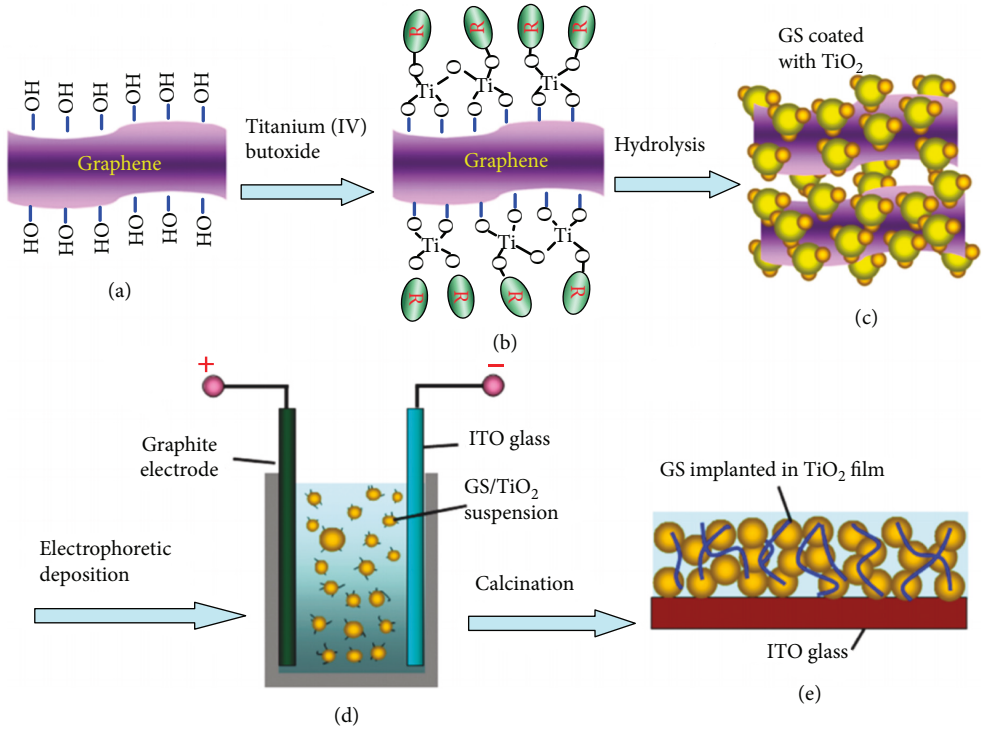

FIGURE 8: Schematic flowchart of in situ incorporation of GS in nanostructured TiO_2 films. (a) GS prepared by chemical exfoliation with residual oxygen-containing functional groups, such as hydroxyl. (b) Schematic of titanium(IV) butoxide grafted on the reduced GS surfaces by chemisorption. (c) Schematic diagram of GS coated with TiO_2 colloids after hydrolysis. (d) Illustration of the electrophoretic deposition process used to prepare GS/TiO_2 composite films. (e) Schematic representation of the structure of the GS/TiO_2 composite film after calcination [147].

DSSC. It was reported that graphene has the ability to work as photosensitizer because charge injection from the graphene material to TiO_2 can occur. However, the performance of graphene in this role is poor. Nevertheless, they have recently shown promise in hot injection [158], showing the promising ability to overtake the Shockley-Queisser efficiency limit inherent to current device structures.

Yan et al. fabricated DSSC using graphene material photosensitizers for the first time [159]. The graphene quantum dots (GQDs) which have a diameter ranging from 1 to 30 nm and had an absorption maximum at 591 nm were employed in this device. The extinction coefficient is $10^5\,M^{-1}\,cm^{-1}$, which is almost an order of magnitude higher than N719. Figure 10 shows the employed strategy to make large graphene quantum dots soluble. In addition to that, the HOMO level was found lesser than the iodide/triiodide redox potential and the LUMO level was higher than the TiO_2 conduction band which suggested that both injection of electron and dye regeneration are possible. It was also proved by the same group that controlling the size of the molecule can tune the bandgap of GQD and changing its functionalization can tune the redox potential [160].

Zamiri and Bagheri also tried to use the combined effect of graphene material and quantum-sized properties for increasing the DSSC efficiency [161]. GQD has a few-graphene-layer size of 100 nm. They are the combination of unique properties of quantum-sized dots and graphene. At the edge, GQDs have very good functional groups, because of which they have an amazing water solubility. By putting multiple coatings of the ZnO nanoparticles on the FTO glasses and also then immersing it in N-719 and GQDs, the effect of the thickness of ZnO nanoparticles on the performance of the DSSC was studied. The I-V tests confirmed that photoanodes with 40 μm thickness show the highest efficiency because with increasing thickness, more photosensitizer molecules present in the semiconductor layer for absorbing sunlight. To study the effect of the various photosensitizers on ZnO photoanode, it was immersed in different photosensitizers for different times. The I-V test shows that if the immersion time is longer, more photosensitizers will be absorbed, which is helpful in increasing the light harvesting efficiency, which ultimately results in increasing efficiency of DSSC.

Esmaeili and Gaznagi tried to add graphene in those traditional sensitizers to improve efficiency [162]. They made two samples for the experiment. In the first sample, they just added graphene into the TiO_2 blocking layer, and in the second sample, they added graphene in the ruthenium-based dye solution as well. The authors demonstrated that loading graphene within the lonely blocking layer and the TiO_2 paste and dye-deposited blocking layer increases the conversion efficiency, charge collection efficiency, Hall carrier concentration, mobility, etc. Those enhancements were attributed to the increased carrier concentration, improved charge transfer, and diminished charge recombination due to the existence of graphene-functionalized interfaces. Perhaps the

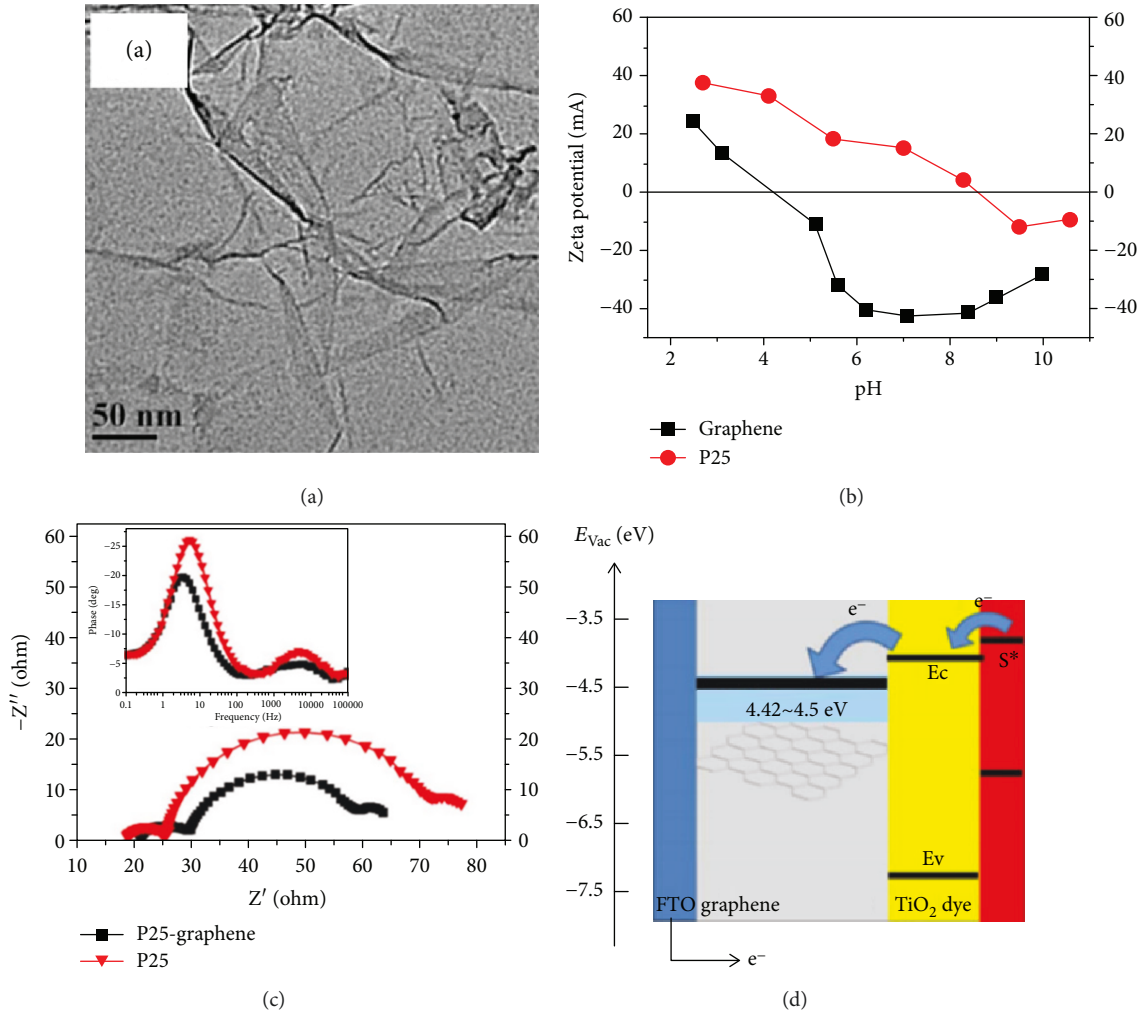

Figure 9: (a) TEM image of the graphene dispersed by Nafion. (b) Zeta potential as a function of pH for Nafion-functionalized graphene and P25. (c) EIS of DSSCs with P25 and P25-graphene electrodes. The inset displays the Bode phase of two films. (d) Schematic diagram for energy band matching [156].

largest role of graphene materials as a DSSC sensitizer would be in a scenario which took advantage of the quantum effects and allowed for ultrafast injection in order to overcome intrinsic limitations to conventional devices.

3. Conclusion and Outlook

As a novel photovoltaic technology, dye-sensitized solar cells (DSSCs) have the potential to compete with traditional solar cells. Compared with silicon solar cells, they are insensitive to impurities in the fabrication process, which accelerates a transition from the research laboratory to the mass production line. Graphene, emerging as one the most unique materials, has been recently explored extensively in DSSC to increase the efficiency and reduce the cost. Graphene has been widely explored in DSSCs as photoelectrodes. It shows great potential to change the solar industry in terms of financially and performance as well. Considering the photoelectrode, it is believed that a correct amount of graphene addition may really enhance the photocurrent in particular cases. Based on the reported results, it is very much evident that graphene materials will play a key role in enhancing the efficiency of the DSSCs. Nevertheless, as research progresses, we should always remember that graphene could have various properties according to their different manufacturing processes and each may be beneficial to different areas in a solar cell. A next stage of research, to bring graphene materials to a higher relevance in the DSSC community, would be to study whether improvements discussed within this review can be carried over to the current best-in-class devices.

Conflicts of Interest

The authors declare no competing financial interest.

Acknowledgments

K.P., S.R., and W.W. thank the support from Wichita State University. H.W. thanks the support from Conn Center for Renewable Energy Research and University of Louisville.

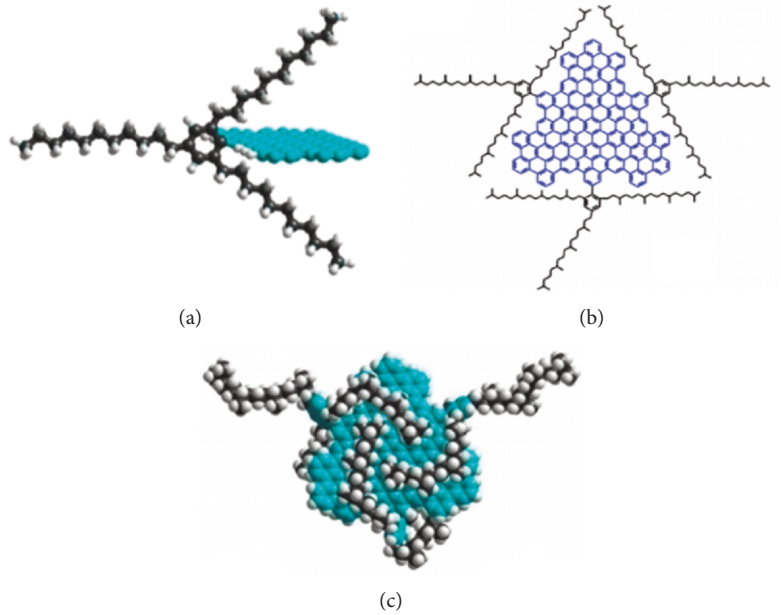

Figure 10: Strategy to make large graphene quantum dots soluble. (a) Attaching 1,3,5-trialkyl phenyl moieties (marked black) covalently to the edge of graphene (blue) to shield the graphenes from one another in three dimensions. Hydrogen atoms are marked white. (b) Molecular structure of graphene quantum dot 1, containing a graphene moiety with 168 conjugated carbon atoms. The graphene moiety is marked blue and the three solubilizing groups black. (c) A theoretically energy-minimized configuration of 1 in vacuum, showing the three-dimensional enclosure of the graphene core by the alkyl chains (black) [159].

References

[1] M. Wang, A. M. Anghel, B. Marsan et al., "CoS supersedes Pt as efficient electrocatalyst for triiodide reduction in dye-sensitized solar cells," *Journal of the American Chemical Society*, vol. 131, no. 44, pp. 15976-15977, 2009.

[2] W. Wei, H. Wang, and Y. H. Hu, "A review on PEDOT-based counter electrodes for dye-sensitized solar cells," *International Journal of Energy Research*, vol. 38, no. 9, pp. 1099–1111, 2014.

[3] M. Grätzel, "Dye-sensitized solar cells," *Journal of Photochemistry and Photobiology C: Photochemistry Reviews*, vol. 4, no. 2, pp. 145–153, 2003.

[4] W. Wei, H. Wang, and Y. H. Hu, "Unusual particle-size-induced promoter-to-poison transition of ZrN in counter electrodes for dye-sensitized solar cells," *Journal of Materials Chemistry A*, vol. 1, no. 45, pp. 14350–14357, 2013.

[5] X. Fang, T. Ma, G. Guan, M. Akiyama, T. Kida, and E. Abe, "Effect of the thickness of the Pt film coated on a counter electrode on the performance of a dye-sensitized solar cell," *Journal of Electroanalytical Chemistry*, vol. 570, no. 2, pp. 257–263, 2004.

[6] S.-S. Kim, Y.-C. Nah, Y.-Y. Noh, J. Jo, and D.-Y. Kim, "Electrodeposited Pt for cost-efficient and flexible dye-sensitized solar cells," *Electrochimica Acta*, vol. 51, no. 18, pp. 3814–3819, 2006.

[7] Y. H. Hu and W. Wei, *2.6 Dye-Sensitized Materials, in Comprehensive Energy Systems*, I. Dincer, Ed., Elsevier, Oxford, 2018.

[8] M. K. Nazeeruddin, P. Péchy, T. Renouard et al., "Engineering of efficient panchromatic sensitizers for nanocrystalline TiO_2-based solar cells," *Journal of the American Chemical Society*, vol. 123, no. 8, pp. 1613–1624, 2001.

[9] C.-Y. Chen, M. Wang, J. Y. Li et al., "Highly efficient light-harvesting ruthenium sensitizer for thin-film dye-sensitized solar cells," *ACS Nano*, vol. 3, no. 10, pp. 3103–3109, 2009.

[10] M. Grätzel, "Perspectives for dye-sensitized nanocrystalline solar cells," *Progress in Photovoltaics: Research and Applications*, vol. 8, no. 1, pp. 171–185, 2000.

[11] M. Grätzel, "Conversion of sunlight to electric power by nanocrystalline dye-sensitized solar cells," *Journal of Photochemistry and Photobiology A: Chemistry*, vol. 164, no. 1-3, pp. 3–14, 2004.

[12] J. H. Park, T. W. Lee, and M. G. Kang, "Growth, detachment and transfer of highly-ordered TiO_2 nanotube arrays: use in dye-sensitized solar cells," *Chemical Communications*, vol. 25, no. 25, pp. 2867–2869, 2008.

[13] S. Hore, C. Vetter, R. Kern, H. Smit, and A. Hinsch, "Influence of scattering layers on efficiency of dye-sensitized solar cells," *Solar Energy Materials and Solar Cells*, vol. 90, no. 9, pp. 1176–1188, 2006.

[14] A. Hagfeldt and M. Grätzel, "Molecular photovoltaics," *Accounts of Chemical Research*, vol. 33, no. 5, pp. 269–277, 2000.

[15] J.-C. Chou, C. H. Huang, Y. J. Lin et al., "The influence of different annealing temperatures on graphene-modified TiO_2 for dye-sensitized solar cell," *IEEE Transactions on Nanotechnology*, vol. 15, no. 2, pp. 164–170, 2016.

[16] A. K. Chandiran, M. Abdi-Jalebi, M. K. Nazeeruddin, and M. Grätzel, "Analysis of electron transfer properties of ZnO and TiO_2 photoanodes for dye-sensitized solar cells," *ACS Nano*, vol. 8, no. 3, pp. 2261–2268, 2014.

[17] A. Banik, M. S. Ansari, T. K. Sahu, and M. Qureshi, "Understanding the role of silica nanospheres with their light scattering and energy barrier properties in enhancing the photovoltaic performance of ZnO based solar cells," *Physical*

Chemistry Chemical Physics, vol. 18, no. 40, pp. 27818–27828, 2016.

[18] M. Bavir and A. Fattah, "An investigation and simulation of the graphene performance in dye-sensitized solar cell," *Optical and Quantum Electronics*, vol. 48, no. 12, 2016.

[19] M. H. Habibi, M. Mardani, M. Habibi, and M. Zendehdel, "Enhanced photovoltage (Voc) of nano-structured zinc tin oxide (ZTO) working electrode prepared by a green hydrothermal route for dye-sensitized solar cell (DSSC)," *Journal of Materials Science: Materials in Electronics*, vol. 28, no. 4, pp. 3789–3795, 2017.

[20] F. I. Lai, J. F. Yang, and S. Y. Kuo, "Efficiency enhancement of dye-sensitized solar cells' performance with ZnO nanorods grown by low-temperature hydrothermal reaction," *Materials*, vol. 8, no. 12, pp. 8860–8867, 2015.

[21] S. Y. Lee and S. H. Kim, "Deposition of zinc oxide photoelectrode using plasma enhanced chemical vapor deposition for dye-sensitized solar cells," *Journal of Nanoscience and Nanotechnology*, vol. 14, no. 12, pp. 9272–9278, 2014.

[22] C. W. Ma, C. M. Chang, P. C. Huang, and Y. J. Yang, "Sea-urchin-like ZnO nanoparticle film for dye-sensitized solar cells," *Journal of Nanomaterials*, vol. 2015, Article ID 679474, 6 pages, 2015.

[23] S. A. Mahmoud and O. A. Fouad, "Synthesis and application of zinc/tin oxide nanostructures in photocatalysis and dye sensitized solar cells," *Solar Energy Materials and Solar Cells*, vol. 136, pp. 38–43, 2015.

[24] P. Pandey, M. R. Parra, F. Z. Haque, and R. Kurchania, "Effects of annealing temperature optimization on the efficiency of ZnO nanoparticles photoanode based dye sensitized solar cells," *Journal of Materials Science: Materials in Electronics*, vol. 28, no. 2, pp. 1537–1545, 2017.

[25] A. Amala Rani and S. Ernest, "Enhancement of efficiency in dye-sensitized solar cell using spray deposited Ga doped ZnO thin films," *Journal of Materials Science: Materials in Electronics*, vol. 26, no. 2, pp. 762–768, 2015.

[26] Z. Zarghami, M. Ramezani, and K. Motevalli, "Zno nanorods/nanoparticles: novel hydrothermal synthesis, characterization and formation mechanism for increasing the efficiency of dye-sensitized solar cells," *Journal of Cluster Science*, vol. 27, no. 4, pp. 1451–1462, 2016.

[27] L. Bahadur and S. Kushwaha, "Structural and optical properties of tripod-like ZnO thin film and its application in dye-sensitized solar cell," *Journal of Solid State Electrochemistry*, vol. 17, no. 7, pp. 2001–2008, 2013.

[28] M. H. Habibi, B. Karimi, M. Zendehdel, and M. Habibi, "Fabrication, characterization of two nano-composite CuO-ZnO working electrodes for dye-sensitized solar cell," *Spectrochimica Acta Part A: Molecular and Biomolecular Spectroscopy*, vol. 116, pp. 374–380, 2013.

[29] M. Kaur and N. K. Verma, "Study on $CaCO_3$-coated ZnO nanoparticles based dye sensitized solar cell," *Journal of Materials Science: Materials in Electronics*, vol. 24, no. 12, pp. 4980–4986, 2013.

[30] M. Kaur and N. K. Verma, "Performance of Eu2O3 coated ZnO nanoparticles-based DSSC," *Journal of Materials Science: Materials in Electronics*, vol. 24, no. 9, pp. 3617–3623, 2013.

[31] Y. R. Kim, J. Y. Park, D. K. Lee, K. S. Ahn, and J. H. Kim, "Dye-sensitized solar cells composed of well-aligned ZnO nanorod array grown with chemical bath deposition method as the photo-electrode," *Molecular Crystals and Liquid Crystals*, vol. 597, no. 1, pp. 120–127, 2014.

[32] S. Kushwaha and L. Bahadur, "Studies of structural and morphological characteristics of flower-like ZnO thin film and its application as photovoltaic material," *Optik*, vol. 124, no. 22, pp. 5696–5701, 2013.

[33] H. Li, J. Bai, B. Feng et al., "Dye-sensitized solar cells with a tri-layer ZnO photo-electrode," *Journal of Alloys and Compounds*, vol. 578, pp. 507–511, 2013.

[34] C. J. Raj, K. Prabakar, S. N. Karthick, K. V. Hemalatha, M. K. Son, and H. J. Kim, "Banyan root structured mg-doped ZnO photoanode dye-sensitized solar cells," *Journal of Physical Chemistry C*, vol. 117, no. 6, pp. 2600–2607, 2013.

[35] H. Wang, H. Li, J. Wang, J. Wu, and M. Liu, "Influence of applied voltage on anodized TiO_2 nanotube arrays and their performance on dye sensitized solar cells," *Journal of Nanoscience and Nanotechnology*, vol. 13, no. 6, pp. 4183–4188, 2013.

[36] K. Wu, Y. Yu, K. Shen, C. Xia, and D. Wang, "Effect of ultra-thin ZnO coating layer on the device performance of TiO_2 dye sensitized solar cell," *Solar Energy*, vol. 94, pp. 195–201, 2013.

[37] K. S. Novoselov, A. K. Geim, S. V. Morozov et al., "Electric field effect in atomically thin carbon films," *Science*, vol. 306, no. 5696, pp. 666–669, 2004.

[38] K. S. Novoselov, A. K. Geim, S. V. Morozov et al., "Two-dimensional gas of massless Dirac fermions in graphene," *Nature*, vol. 438, no. 7065, pp. 197–200, 2005.

[39] A. K. Geim and K. S. Novoselov, "The rise of graphene," *Nature Materials*, vol. 6, no. 3, pp. 183–191, 2007.

[40] A. K. Geim, "Graphene: status and prospects," *Science*, vol. 324, no. 5934, pp. 1530–1534, 2009.

[41] R. Zan, Q. M. Ramasse, U. Bangert, and K. S. Novoselov, "Graphene reknits its holes," *Nano Letters*, vol. 12, no. 8, pp. 3936–3940, 2012.

[42] K. I. Ho, M. Boutchich, C. Y. Su et al., "A self-aligned high-mobility graphene transistor: decoupling the channel with fluorographene to reduce scattering," *Advanced Materials*, vol. 27, no. 41, pp. 6519–6525, 2015.

[43] K. S. Novoselov, D. Jiang, F. Schedin et al., "Two-dimensional atomic crystals," *Proceedings of the National Academy of Sciences of the United States of America*, vol. 102, no. 30, pp. 10451–10453, 2005.

[44] D. C. Elias, R. R. Nair, T. M. G. Mohiuddin et al., "Control of graphene's properties by reversible hydrogenation: evidence for graphane," *Science*, vol. 323, no. 5914, pp. 610–613, 2009.

[45] J. Theerthagiri, A. R. Senthil, J. Madhavan, and T. Maiyalagan, "Recent progress in non-platinum counter electrode materials for dye-sensitized solar cells," *ChemElectroChem*, vol. 2, no. 7, pp. 928–945, 2015.

[46] M. Toivola, J. Halme, K. Miettunen, K. Aitola, and P. D. Lund, "Nanostructured dye solar cells on flexible substrates—review," *International Journal of Energy Research*, vol. 33, no. 13, pp. 1145–1160, 2009.

[47] S. Latil and L. Henrard, "Charge carriers in few-layer graphene films," *Physical Review Letters*, vol. 97, no. 3, article 036803, 2006.

[48] T. Mueller, F. Xia, and P. Avouris, "Graphene photodetectors for high-speed optical communications," *Nature Photonics*, vol. 4, no. 5, pp. 297–301, 2010.

[49] W. Wei and Y. H. Hu, "Highly conductive Na-embedded carbon nanowalls for hole-transport-material-free perovskite solar cells without metal electrodes," *Journal of Materials Chemistry A*, vol. 5, no. 46, pp. 24126–24130, 2017.

[50] W. Wei, K. Sun, and Y. H. Hu, "Synthesis of mesochannel carbon nanowall material from CO_2 and its excellent performance for perovskite solar cells," *Industrial & Engineering Chemistry Research*, vol. 56, no. 7, pp. 1803–1809, 2017.

[51] W. Wei, L. Chang, K. Sun et al., "The bright future for electrode materials of energy devices: highly conductive porous Na-embedded carbon," *Nano Letters*, vol. 16, no. 12, pp. 8029–8033, 2016.

[52] W. Wei, B. Hu, F. Jin et al., "Potassium-chemical synthesis of 3D graphene from CO_2 and its excellent performance in HTM-free perovskite solar cells," *Journal of Materials Chemistry A*, vol. 5, no. 17, pp. 7749–7752, 2017.

[53] W. Wei and Y. H. Hu, "Synthesis of carbon nanomaterials for dye-sensitized solar cells," *International Journal of Energy Research*, vol. 39, no. 6, pp. 842–850, 2015.

[54] W. Wei and Y. H. Hu, "3D MoS2/graphene hybrid layer materials as counter electrodes for dye-sensitized solar cells," in *Catalysis: Volume 28*, pp. 268–280, Royal Society of Chemistry, 2016.

[55] W. Wei, K. Sun, and Y. H. Hu, "Synthesis of 3D cauliflower-fungus-like graphene from CO_2 as a highly efficient counter electrode material for dye-sensitized solar cells," *Journal of Materials Chemistry A*, vol. 2, no. 40, pp. 16842–16846, 2014.

[56] W. Wei, K. Sun, and Y. H. Hu, "Direct conversion of CO_2 to 3D graphene and its excellent performance for dye-sensitized solar cells with 10% efficiency," *Journal of Materials Chemistry A*, vol. 4, no. 31, pp. 12054–12057, 2016.

[57] G. Yue, J. Y. Lin, S. Y. Tai, Y. Xiao, and J. Wu, "A catalytic composite film of MoS_2/graphene flake as a counter electrode for Pt-free dye-sensitized solar cells," *Electrochimica Acta*, vol. 85, pp. 162–168, 2012.

[58] N. Huang, G. Li, Z. Xia et al., "Solution-processed relatively pure MoS_2 nanoparticles in-situ grown on graphite paper as an efficient FTO-free counter electrode for dye-sensitized solar cells," *Electrochimica Acta*, vol. 235, pp. 182–190, 2017.

[59] Y. Li, H. Wang, Q. Feng, G. Zhou, and Z. S. Wang, "Reduced graphene oxide-TaON composite as a high-performance counter electrode for $Co(bpy)_3^{3+/2+}$-mediated dye-sensitized solar cells," *ACS Applied Materials & Interfaces*, vol. 5, no. 16, pp. 8217–8224, 2013.

[60] D. W. Zhang, X. D. Li, H. B. Li et al., "Graphene-based counter electrode for dye-sensitized solar cells," *Carbon*, vol. 49, no. 15, pp. 5382–5388, 2011.

[61] K. S. Kim, Y. Zhao, H. Jang et al., "Large-scale pattern growth of graphene films for stretchable transparent electrodes," *Nature*, vol. 457, no. 7230, pp. 706–710, 2009.

[62] X. Li, W. Cai, J. An et al., "Large-area synthesis of high-quality and uniform graphene films on copper foils," *Science*, vol. 324, no. 5932, pp. 1312–1314, 2009.

[63] P. W. Sutter, J.-I. Flege, and E. A. Sutter, "Epitaxial graphene on ruthenium," *Nature Materials*, vol. 7, no. 5, pp. 406–411, 2008.

[64] N. Xiao, X. Dong, L. Song et al., "Enhanced thermopower of graphene films with oxygen plasma treatment," *ACS Nano*, vol. 5, no. 4, pp. 2749–2755, 2011.

[65] C. Berger, Z. Song, T. Li et al., "Ultrathin epitaxial graphite: 2D electron gas properties and a route toward graphene-based nanoelectronics," *The Journal of Physical Chemistry B*, vol. 108, no. 52, pp. 19912–19916, 2004.

[66] K. V. Emtsev, A. Bostwick, K. Horn et al., "Towards wafer-size graphene layers by atmospheric pressure graphitization of silicon carbide," *Nature Materials*, vol. 8, no. 3, pp. 203–207, 2009.

[67] M. Choucair, P. Thordarson, and J. A. Stride, "Gram-scale production of graphene based on solvothermal synthesis and sonication," *Nature Nanotechnology*, vol. 4, no. 1, pp. 30–33, 2009.

[68] X. Wang, L. Zhi, N. Tsao, Ž. Tomović, J. Li, and K. Müllen, "Transparent carbon films as electrodes in organic solar cells," *Angewandte Chemie International Edition*, vol. 47, no. 16, pp. 2990–2992, 2008.

[69] X. Yan, X. Cui, and L.-s. Li, "Synthesis of large, stable colloidal graphene quantum dots with tunable size," *Journal of the American Chemical Society*, vol. 132, no. 17, pp. 5944-5945, 2010.

[70] N. Liu, F. Luo, H. Wu, Y. Liu, C. Zhang, and J. Chen, "One--step ionic-liquid-assisted electrochemical synthesis of ionic-liquid-functionalized graphene sheets directly from graphite," *Advanced Functional Materials*, vol. 18, no. 10, pp. 1518–1525, 2008.

[71] M. Lotya, Y. Hernandez, P. J. King et al., "Liquid phase production of graphene by exfoliation of graphite in surfactant/-water solutions," *Journal of the American Chemical Society*, vol. 131, no. 10, pp. 3611–3620, 2009.

[72] Y. Hernandez, V. Nicolosi, M. Lotya et al., "High-yield production of graphene by liquid-phase exfoliation of graphite," *Nature Nanotechnology*, vol. 3, no. 9, pp. 563–568, 2008.

[73] D. Li, M. B. Müller, S. Gilje, R. B. Kaner, and G. G. Wallace, "Processable aqueous dispersions of graphene nanosheets," *Nature Nanotechnology*, vol. 3, no. 2, pp. 101–105, 2008.

[74] X. Zhou, X. Huang, X. Qi et al., "In situ synthesis of metal nanoparticles on single-layer graphene oxide and reduced graphene oxide surfaces," *The Journal of Physical Chemistry C*, vol. 113, no. 25, pp. 10842–10846, 2009.

[75] W. S. Hummers Jr and R. E. Offeman, "Preparation of graphitic oxide," *Journal of the American Chemical Society*, vol. 80, no. 6, pp. 1339–1339, 1958.

[76] A. Lerf, H. He, M. Forster, and J. Klinowski, "Structure of graphite oxide revisited," *The Journal of Physical Chemistry B*, vol. 102, no. 23, pp. 4477–4482, 1998.

[77] W. Gao, L. B. Alemany, L. Ci, and P. M. Ajayan, "New insights into the structure and reduction of graphite oxide," *Nature Chemistry*, vol. 1, no. 5, pp. 403–408, 2009.

[78] S. Wu, Z. Yin, Q. He, G. Lu, X. Zhou, and H. Zhang, "Electrochemical deposition of Cl-doped n-type Cu_2O on reduced graphene oxide electrodes," *Journal of Materials Chemistry*, vol. 21, no. 10, pp. 3467–3470, 2011.

[79] S. Agarwal, X. Zhou, F. Ye et al., "Interfacing live cells with nanocarbon substrates," *Langmuir*, vol. 26, no. 4, pp. 2244–2247, 2010.

[80] Y. Yang, Z. Liu, Z. Yin et al., "Rod-coating all-solution fabrication of double functional graphene oxide films for flexible alternating current (AC)-driven light-emitting diodes," *RSC Advances*, vol. 4, no. 98, pp. 55671–55676, 2014.

[81] W. Hu, C. Peng, W. Luo et al., "Graphene-based antibacterial paper," *ACS Nano*, vol. 4, no. 7, pp. 4317–4323, 2010.

[82] Y. Wang, Z. Shi, Y. Huang et al., "Supercapacitor devices based on graphene materials," *The Journal of Physical Chemistry C*, vol. 113, no. 30, pp. 13103–13107, 2009.

[83] X. Fan, W. Peng, Y. Li et al., "Deoxygenation of exfoliated graphite oxide under alkaline conditions: a green route to graphene preparation," *Advanced Materials*, vol. 20, no. 23, pp. 4490–4493, 2008.

[84] V. Dua, S. P. Surwade, S. Ammu et al., "All-organic vapor sensor using inkjet-printed reduced graphene oxide," *Angewandte Chemie International Edition*, vol. 49, no. 12, pp. 2154–2157, 2010.

[85] J. Liu, S. Fu, B. Yuan, Y. Li, and Z. Deng, "Toward a universal "adhesive nanosheet" for the assembly of multiple nanoparticles based on a protein-induced reduction/decoration of graphene oxide," *Journal of the American Chemical Society*, vol. 132, no. 21, pp. 7279–7281, 2010.

[86] Q. He, S. Wu, S. Gao et al., "Transparent, flexible, all-reduced graphene oxide thin film transistors," *ACS Nano*, vol. 5, no. 6, pp. 5038–5044, 2011.

[87] G. Williams, B. Seger, and P. V. Kamat, "TiO_2-graphene nanocomposites. UV-assisted photocatalytic reduction of graphene oxide," *ACS Nano*, vol. 2, no. 7, pp. 1487–1491, 2008.

[88] W. Wei, T. He, X. Teng et al., "Nanocomposites of graphene oxide and upconversion rare-earth nanocrystals with superior optical limiting performance," *Small*, vol. 8, no. 14, pp. 2271–2276, 2012.

[89] Y. Matsumoto, M. Koinuma, S. Y. Kim et al., "Simple photoreduction of graphene oxide nanosheet under mild conditions," *ACS Applied Materials & Interfaces*, vol. 2, no. 12, pp. 3461–3466, 2010.

[90] Y. H. Ng, A. Iwase, A. Kudo, and R. Amal, "Reducing graphene oxide on a visible-light $BiVO_4$ photocatalyst for an enhanced photoelectrochemical water splitting," *The Journal of Physical Chemistry Letters*, vol. 1, no. 17, pp. 2607–2612, 2010.

[91] H. M. A. Hassan, V. Abdelsayed, A. E. R. S. Khder et al., "Microwave synthesis of graphene sheets supporting metal nanocrystals in aqueous and organic media," *Journal of Materials Chemistry*, vol. 19, no. 23, pp. 3832–3837, 2009.

[92] S. Dubin, S. Gilje, K. Wang et al., "A one-step, solvothermal reduction method for producing reduced graphene oxide dispersions in organic solvents," *ACS Nano*, vol. 4, no. 7, pp. 3845–3852, 2010.

[93] C. Mattevi, G. Eda, S. Agnoli et al., "Evolution of electrical, chemical, and structural properties of transparent and conducting chemically derived graphene thin films," *Advanced Functional Materials*, vol. 19, no. 16, pp. 2577–2583, 2009.

[94] S. Mao, G. Lu, K. Yu, Z. Bo, and J. Chen, "Specific protein detection using thermally reduced graphene oxide sheet decorated with gold nanoparticle-antibody conjugates," *Advanced Materials*, vol. 22, no. 32, pp. 3521–3526, 2010.

[95] Y. Zhu, M. D. Stoller, W. Cai et al., "Exfoliation of graphite oxide in propylene carbonate and thermal reduction of the resulting graphene oxide platelets," *ACS Nano*, vol. 4, no. 2, pp. 1227–1233, 2010.

[96] J. Wu, M. Agrawal, H. A. Becerril et al., "Organic light-emitting diodes on solution-processed graphene transparent electrodes," *ACS Nano*, vol. 4, no. 1, pp. 43–48, 2009.

[97] H. A. Becerril, J. Mao, Z. Liu, R. M. Stoltenberg, Z. Bao, and Y. Chen, "Evaluation of solution-processed reduced graphene oxide films as transparent conductors," *ACS Nano*, vol. 2, no. 3, pp. 463–470, 2008.

[98] C. D. Zangmeister, "Preparation and evaluation of graphite oxide reduced at 220 °C," *Chemistry of Materials*, vol. 22, no. 19, pp. 5625–5629, 2010.

[99] V. Abdelsayed, S. Moussa, H. M. Hassan, H. S. Aluri, M. M. Collinson, and M. S. el-Shall, "Photothermal deoxygenation of graphite oxide with laser excitation in solution and graphene-aided increase in water temperature," *The Journal of Physical Chemistry Letters*, vol. 1, no. 19, pp. 2804–2809, 2010.

[100] L. J. Cote, R. Cruz-Silva, and J. Huang, "Flash reduction and patterning of graphite oxide and its polymer composite," *Journal of the American Chemical Society*, vol. 131, no. 31, pp. 11027–11032, 2009.

[101] Z. Wang, X. Zhou, J. Zhang, F. Boey, and H. Zhang, "Direct electrochemical reduction of single-layer graphene oxide and subsequent functionalization with glucose oxidase," *The Journal of Physical Chemistry C*, vol. 113, no. 32, pp. 14071–14075, 2009.

[102] M. Zhou, Y. Wang, Y. Zhai et al., "Controlled synthesis of large-area and patterned electrochemically reduced graphene oxide films," *Chemistry – A European Journal*, vol. 15, no. 25, pp. 6116–6120, 2009.

[103] G. K. Ramesha and S. Sampath, "Electrochemical reduction of oriented graphene oxide films: an in situ Raman spectroelectrochemical study," *The Journal of Physical Chemistry C*, vol. 113, no. 19, pp. 7985–7989, 2009.

[104] X. Qi, K. Y. Pu, H. Li et al., "Amphiphilic graphene composites," *Angewandte Chemie International Edition*, vol. 49, no. 49, pp. 9426–9429, 2010.

[105] M. A. Raj and S. A. John, "Fabrication of electrochemically reduced graphene oxide films on glassy carbon electrode by self-assembly method and their electrocatalytic application," *The Journal of Physical Chemistry C*, vol. 117, no. 8, pp. 4326–4335, 2013.

[106] E. C. Salas, Z. Sun, A. Lüttge, and J. M. Tour, "Reduction of graphene oxide via bacterial respiration," *ACS Nano*, vol. 4, no. 8, pp. 4852–4856, 2010.

[107] R. Krishna, D. M. Fernandes, E. Venkataramana et al., "Improved reduction of graphene oxide," *Materials Today: Proceedings*, vol. 2, no. 1, pp. 423–430, 2015.

[108] G. Eda, Y. Y. Lin, C. Mattevi et al., "Blue photoluminescence from chemically derived graphene oxide," *Advanced Materials*, vol. 22, no. 4, pp. 505–509, 2010.

[109] S. Stankovich, D. A. Dikin, G. H. B. Dommett et al., "Graphene-based composite materials," *Nature*, vol. 442, no. 7100, pp. 282–286, 2006.

[110] D. Vanmaekelbergh, "Self-assembly of colloidal nanocrystals as route to novel classes of nanostructured materials," *Nano Today*, vol. 6, no. 4, pp. 419–437, 2011.

[111] H. Bai, C. Li, X. Wang, and G. Shi, "On the gelation of graphene oxide," *The Journal of Physical Chemistry C*, vol. 115, no. 13, pp. 5545–5551, 2011.

[112] H. Bai, C. Li, X. Wang, and G. Shi, "A pH-sensitive graphene oxide composite hydrogel," *Chemical Communications*, vol. 46, no. 14, pp. 2376–2378, 2010.

[113] O. C. Compton, Z. An, K. W. Putz et al., "Additive-free hydrogelation of graphene oxide by ultrasonication," *Carbon*, vol. 50, no. 10, pp. 3399–3406, 2012.

[114] Y. Xu, Q. Wu, Y. Sun, H. Bai, and G. Shi, "Three-dimensional self-assembly of graphene oxide and DNA into multifunctional hydrogels," *ACS Nano*, vol. 4, no. 12, pp. 7358–7362, 2010.

[115] H.-P. Cong, X. C. Ren, P. Wang, and S. H. Yu, "Macroscopic multifunctional graphene-based hydrogels and aerogels by a metal ion induced self-assembly process," *ACS Nano*, vol. 6, no. 3, pp. 2693–2703, 2012.

[116] Z.-S. Wu, S. Yang, Y. Sun, K. Parvez, X. Feng, and K. Müllen, "3D nitrogen-doped graphene aerogel-supported Fe_3O_4 nanoparticles as efficient electrocatalysts for the oxygen reduction reaction," *Journal of the American Chemical Society*, vol. 134, no. 22, pp. 9082–9085, 2012.

[117] Y. Chang, J. Li, B. Wang et al., "Synthesis of 3D nitrogen-doped graphene/Fe_3O_4 by a metal ion induced self-assembly process for high-performance Li-ion batteries," *Journal of Materials Chemistry A*, vol. 1, no. 46, pp. 14658–14665, 2013.

[118] S. Sun and P. Wu, "A one-step strategy for thermal- and pH-responsive graphene oxide interpenetrating polymer hydrogel networks," *Journal of Materials Chemistry*, vol. 21, no. 12, pp. 4095–4097, 2011.

[119] P. M. Sudeep, T. N. Narayanan, A. Ganesan et al., "Covalently interconnected three-dimensional graphene oxide solids," *ACS Nano*, vol. 7, no. 8, pp. 7034–7040, 2013.

[120] H. Sun, Z. Xu, and C. Gao, "Multifunctional, ultra-flyweight, synergistically assembled carbon aerogels," *Advanced Materials*, vol. 25, no. 18, pp. 2554–2560, 2013.

[121] S. Korkut, J. D. Roy-Mayhew, D. M. Dabbs, D. L. Milius, and I. A. Aksay, "High surface area tapes produced with functionalized graphene," *ACS Nano*, vol. 5, no. 6, pp. 5214–5222, 2011.

[122] X. Yang, J. Zhu, L. Qiu, and D. Li, "Bioinspired effective prevention of restacking in multilayered graphene films: towards the next generation of high-performance supercapacitors," *Advanced Materials*, vol. 23, no. 25, pp. 2833–2838, 2011.

[123] F. Liu and T. S. Seo, "A controllable self-assembly method for large-scale synthesis of graphene sponges and free-standing graphene films," *Advanced Functional Materials*, vol. 20, no. 12, pp. 1930–1936, 2010.

[124] K. Sheng, Y. Sun, C. Li, W. Yuan, and G. Shi, "Ultrahigh-rate supercapacitors based on eletrochemically reduced graphene oxide for ac line-filtering," *Scientific Reports*, vol. 2, no. 1, p. 247, 2012.

[125] M. A. Worsley, T. Y. Olson, J. R. I. Lee et al., "High surface area, sp2-cross-linked three-dimensional graphene monoliths," *The Journal of Physical Chemistry Letters*, vol. 2, no. 8, pp. 921–925, 2011.

[126] M. A. Worsley, P. J. Pauzauskie, T. Y. Olson, J. Biener, J. H. Satcher Jr, and T. F. Baumann, "Synthesis of graphene aerogel with high electrical conductivity," *Journal of the American Chemical Society*, vol. 132, no. 40, pp. 14067–14069, 2010.

[127] Z. Chen, W. Ren, L. Gao, B. Liu, S. Pei, and H. M. Cheng, "Three-dimensional flexible and conductive interconnected graphene networks grown by chemical vapour deposition," *Nature Materials*, vol. 10, no. 6, pp. 424–428, 2011.

[128] X. Cao, Y. Shi, W. Shi et al., "Preparation of novel 3D graphene networks for supercapacitor applications," *Small*, vol. 7, no. 22, pp. 3163–3168, 2011.

[129] Z. Chen, W. Ren, B. Liu et al., "Bulk growth of mono- to few-layer graphene on nickel particles by chemical vapor deposition from methane," *Carbon*, vol. 48, no. 12, pp. 3543–3550, 2010.

[130] M. Zhou, T. Lin, F. Huang et al., "Highly conductive porous graphene/ceramic composites for heat transfer and thermal energy storage," *Advanced Functional Materials*, vol. 23, no. 18, pp. 2263–2269, 2013.

[131] G. Ning, Z. Fan, G. Wang, J. Gao, W. Qian, and F. Wei, "Gram-scale synthesis of nanomesh graphene with high surface area and its application in supercapacitor electrodes," *Chemical Communications*, vol. 47, no. 21, pp. 5976–5978, 2011.

[132] X. Xiao, T. E. Beechem, M. T. Brumbach et al., "Lithographically defined three-dimensional graphene structures," *ACS Nano*, vol. 6, no. 4, pp. 3573–3579, 2012.

[133] X. Xiao, J. R. Michael, T. Beechem et al., "Three dimensional nickel–graphene core–shell electrodes," *Journal of Materials Chemistry*, vol. 22, no. 45, pp. 23749–23754, 2012.

[134] R. Wang, Y. Hao, Z. Wang, H. Gong, and J. T. L. Thong, "Large-diameter graphene nanotubes synthesized using Ni nanowire templates," *Nano Letters*, vol. 10, no. 12, pp. 4844–4850, 2010.

[135] S.-M. Yoon, W. M. Choi, H. Baik et al., "Synthesis of multilayer graphene balls by carbon segregation from nickel nanoparticles," *ACS Nano*, vol. 6, no. 8, pp. 6803–6811, 2012.

[136] J.-S. Lee, H. J. Ahn, J. C. Yoon, and J. H. Jang, "Three-dimensional nano-foam of few-layer graphene grown by CVD for DSSC," *Physical Chemistry Chemical Physics*, vol. 14, no. 22, pp. 7938–7943, 2012.

[137] Z. Bo, K. Yu, G. Lu, P. Wang, S. Mao, and J. Chen, "Understanding growth of carbon nanowalls at atmospheric pressure using normal glow discharge plasma-enhanced chemical vapor deposition," *Carbon*, vol. 49, no. 6, pp. 1849–1858, 2011.

[138] K. Yu, P. Wang, G. Lu, K. H. Chen, Z. Bo, and J. Chen, "Patterning vertically oriented graphene sheets for nanodevice applications," *The Journal of Physical Chemistry Letters*, vol. 2, no. 6, pp. 537–542, 2011.

[139] C. S. Rout, A. Kumar, T. S. Fisher, U. K. Gautam, Y. Bando, and D. Golberg, "Synthesis of chemically bonded CNT–graphene heterostructure arrays," *RSC Advances*, vol. 2, no. 22, pp. 8250–8253, 2012.

[140] X. Cao, Z. Yin, and H. Zhang, "Three-dimensional graphene materials: preparation, structures and application in supercapacitors," *Energy & Environmental Science*, vol. 7, no. 6, pp. 1850–1865, 2014.

[141] F. Bonaccorso, Z. Sun, T. Hasan, and A. C. Ferrari, "Graphene photonics and optoelectronics," *Nature Photonics*, vol. 4, no. 9, pp. 611–622, 2010.

[142] X. Wang, L. Zhi, and K. Müllen, "Transparent, conductive graphene electrodes for dye-sensitized solar cells," *Nano Letters*, vol. 8, no. 1, pp. 323–327, 2008.

[143] H. Bi, S. Sun, F. Huang, X. Xie, and M. Jiang, "Direct growth of few-layer graphene films on SiO_2 substrates and their photovoltaic applications," *Journal of Materials Chemistry*, vol. 22, no. 2, pp. 411–416, 2012.

[144] T. Chen, W. Hu, J. Song, G. H. Guai, and C. M. Li, "Interface functionalization of photoelectrodes with graphene for high performance dye-sensitized solar cells," *Advanced Functional Materials*, vol. 22, no. 24, pp. 5245–5250, 2012.

[145] T. Ramanathan, A. A. Abdala, S. Stankovich et al., "Functionalized graphene sheets for polymer nanocomposites," *Nature Nanotechnology*, vol. 3, no. 6, pp. 327–331, 2008.

[146] H. Wang, S. L. Leonard, and Y. H. Hu, "Promoting effect of graphene on dye-sensitized solar cells," *Industrial & Engineering Chemistry Research*, vol. 51, no. 32, pp. 10613–10620, 2012.

[147] Y.-B. Tang, C. S. Lee, J. Xu et al., "Incorporation of graphenes in nanostructured TiO_2 films via molecular grafting for dye-sensitized solar cell application," *ACS Nano*, vol. 4, no. 6, pp. 3482–3488, 2010.

[148] A. du, Y. H. Ng, N. J. Bell, Z. Zhu, R. Amal, and S. C. Smith, "Hybrid graphene/titania nanocomposite: Interface charge transfer, hole doping, and sensitization for visible light response," *The Journal of Physical Chemistry Letters*, vol. 2, no. 8, pp. 894–899, 2011.

[149] J. Liang, G. Zhang, J. Yang, W. Sun, and M. Shi, "TiO_2 hierarchical nanostructures: hydrothermal fabrication and application in dye-sensitized solar cells," *AIP Advances*, vol. 5, no. 1, article 017141, 2015.

[150] N. Yang, J. Zhai, D. Wang, Y. Chen, and L. Jiang, "Two-dimensional graphene bridges enhanced photoinduced charge transport in dye-sensitized solar cells," *ACS Nano*, vol. 4, no. 2, pp. 887–894, 2010.

[151] A. Peigney, C. Laurent, E. Flahaut, R. R. Bacsa, and A. Rousset, "Specific surface area of carbon nanotubes and bundles of carbon nanotubes," *Carbon*, vol. 39, no. 4, pp. 507–514, 2001.

[152] A. Wojcik and P. V. Kamat, "Reduced graphene oxide and porphyrin. An interactive affair in 2-D," *ACS Nano*, vol. 4, no. 11, pp. 6697–6706, 2010.

[153] S. R. Kim, M. K. Parvez, and M. Chhowalla, "UV-reduction of graphene oxide and its application as an interfacial layer to reduce the back-transport reactions in dye-sensitized solar cells," *Chemical Physics Letters*, vol. 483, no. 1-3, pp. 124–127, 2009.

[154] W. Yang, X. Xu, Y. Gao et al., "High-surface-area nanomesh graphene with enriched edge sites as efficient metal-free cathodes for dye-sensitized solar cells," *Nanoscale*, vol. 8, no. 26, pp. 13059–13066, 2016.

[155] F. W. Low, C. W. Lai, and S. B. Abd Hamid, "Study of reduced graphene oxide film incorporated of TiO_2 species for efficient visible light driven dye-sensitized solar cell," *Journal of Materials Science: Materials in Electronics*, vol. 28, no. 4, pp. 3819–3836, 2017.

[156] S. Sun, L. Gao, and Y. Liu, "Enhanced dye-sensitized solar cell using graphene-TiO_2 photoanode prepared by heterogeneous coagulation," *Applied Physics Letters*, vol. 96, no. 8, article 83113, 2010.

[157] B. Kilic and S. Turkdogan, "Fabrication of dye-sensitized solar cells using graphene sandwiched 3D-ZnO nanostructures based photoanode and Pt-free pyrite counter electrode," *Materials Letters*, vol. 193, pp. 195–198, 2017.

[158] K. J. Williams, C. A. Nelson, X. Yan, L. S. Li, and X. Zhu, "Hot electron injection from graphene quantum dots to TiO_2," *ACS Nano*, vol. 7, no. 2, pp. 1388–1394, 2013.

[159] X. Yan, X. Cui, B. Li, and L. S. Li, "Large, solution-processable graphene quantum dots as light absorbers for photovoltaics," *Nano Letters*, vol. 10, no. 5, pp. 1869–1873, 2010.

[160] X. Yan, B. Li, X. Cui, Q. Wei, K. Tajima, and L. S. Li, "Independent tuning of the band gap and redox potential of graphene quantum dots," *The Journal of Physical Chemistry Letters*, vol. 2, no. 10, pp. 1119–1124, 2011.

[161] G. Zamiri and S. Bagheri, "Fabrication of green dye-sensitized solar cell based on ZnO nanoparticles as a photoanode and graphene quantum dots as a photo-sensitizer," *Journal of Colloid and Interface Science*, vol. 511, pp. 318–324, 2018.

[162] A. Esmaeili and S. Gaznagi, "The performance of ruthenium based dye sensitized solar cells in the presence of graphene," *Physica Status Solidi (A)*, vol. 213, no. 12, pp. 3199–3204, 2016.

[163] B. Tang and G. Hu, "Two kinds of graphene-based composites for photoanode applying in dye-sensitized solar cell," *Journal of Power Sources*, vol. 220, pp. 95–102, 2012.

[164] J.-H. Park, S. W. Seo, J. H. Kim et al., "Improved efficiency of dye-sensitized solar cell using graphene-coated Al_2O_3-TiO_2 nanocomposite Photoanode," *Molecular Crystals and Liquid Crystals*, vol. 538, no. 1, pp. 285–291, 2011.

[165] P. Zhu, A. S. Nair, P. Shengjie, Y. Shengyuan, and S. Ramakrishna, "Facile fabrication of TiO_2–graphene composite with enhanced photovoltaic and photocatalytic properties by electrospinning," *ACS Applied Materials & Interfaces*, vol. 4, no. 2, pp. 581–585, 2012.

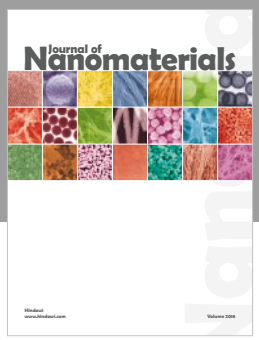

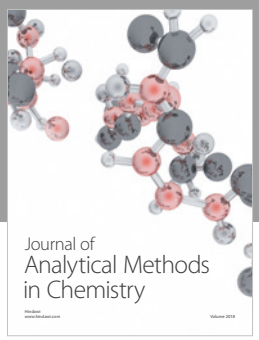

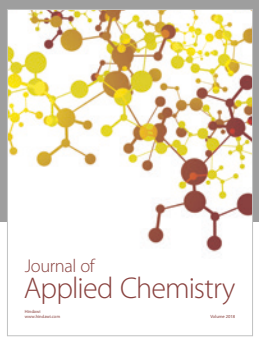

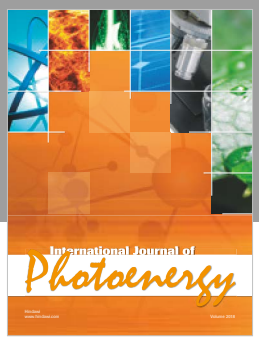

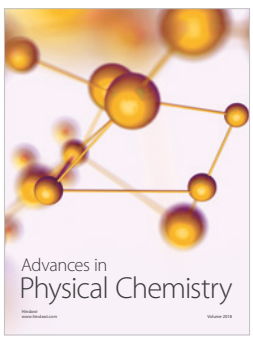

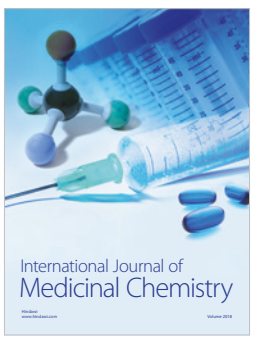

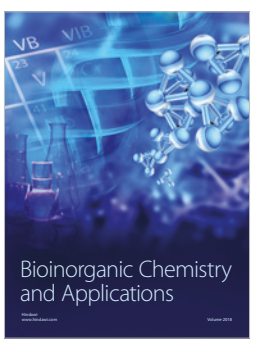

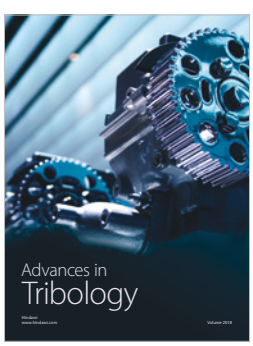

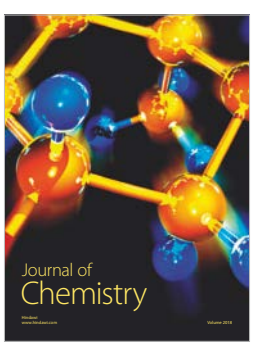

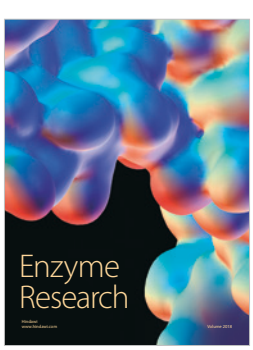

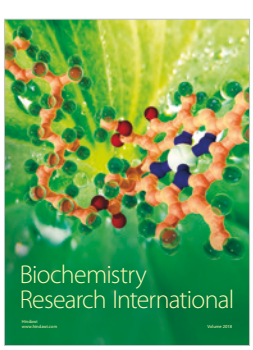

Hindawi

Submit your manuscripts at
www.hindawi.com